Title	Observation of simultaneous oscillations of bunch shape and position caused by odd-harmonic beam loading in the Japan Proton Accelerator Research Complex Rapid Cycling Synchrotron
Author(s)	Yamamoto Masanobu, Nomura Masahiro, Shimada Taihei, Tamura Fumihiko, Hara Keigo, Hasegawa Katsushi, Omori Chihiro, Sugiyama Yasuyuki, Yoshii Masahito
Citation	Progress of Theoretical and Experimental Physics, 2017(11),p.113G01_1-113G01_24
Text Version	Published Journal Article
URL	https://jopss.jaea.go.jp/search/servlet/search?5060736
DOI	https://doi.org/10.1093/ptep/ptx141
Right	© The Author(s) 2017. Published by Oxford University Press on behalf of the Physical Society of Japan. This is an Open Access article distributed under the terms of the Creative Commons Attribution License (http://creativecommons.org/licenses/by/4.0/),which permits unrestricted reuse, distribution, and reproduction in any medium, provided the original work is properly cited.

Observation of simultaneous oscillations of bunch shape and position caused by odd-harmonic beam loading in the Japan Proton Accelerator Research Complex Rapid Cycling Synchrotron

Masanobu Yamamoto[1,*], Masahiro Nomura[1], Taihei Shimada[1], Fumihiko Tamura[1], Keigo Hara[2], Katsushi Hasegawa[2], Chihiro Ohmori[2], Yasuyuki Sugiyama[2], and Masahito Yoshii[2]

[1]*Japan Atomic Energy Agency, 2-4, Shirakata, Tokai Village, Ibaraki 319-1195, Japan*
[2]*High Energy Accelerator Research Organization (KEK), Tsukuba, Ibaraki 305-0801, Japan*
*E-mail: masanobu.yamamoto@j-parc.jp

....
The Japan Proton Accelerator Research Complex Rapid Cycling Synchrotron (RCS) accelerates two particle bunches at a harmonic number of two. The major Fourier components of the beam current are even harmonics. However, the odd harmonics grow and cause a large amount of beam loss, though they are very small at the outset. Beam measurement suggests that the odd harmonic wake voltages promote oscillations not only of the bunch position but also the bunch shape. The oscillations continue because they amplify the odd harmonic beam components. A particle tracking simulation can reproduce these simultaneous oscillations. It is found that the odd harmonic wake voltages lead to severe rf bucket distortion that results in beam loss. In this article, we describe the observation result and the consideration of a mechanism for the bunch behavior caused by the odd harmonics in the RCS.
....
Subject Index   G10

1. Introduction

The Japan Proton Accelerator Research Complex (J-PARC) Rapid Cycling Synchrotron (RCS) accelerates a high-intensity proton beam from 400 MeV to 3 GeV at a repetition rate of 25 Hz. Beam commissioning has progressed successfully, and we have achieved acceleration of a 1 MW-equivalent beam without significant beam loss [1].

A heavy beam loading effect is the most important issue for longitudinal beam motion. A beam loading compensation system using the rf-feedforward method is utilized to cancel the wake voltage in order to achieve stable beam acceleration [2,3]. The rf cavity of the RCS has a broadband impedance to cover a wide frequency range of fundamental acceleration voltage and to generate the second harmonic voltage in the same cavity [4,5]. Consequently, the beam loading compensation system is designed to cope with the multi-harmonics for the harmonic numbers of $h = 1$–6 based on a revolution frequency, which covers the cavity impedance bandwidth sufficiently.

The RCS accelerates two particle bunches at the harmonic number $h = 2$. The major Fourier components of the beam current are even harmonics if the electric charges and shapes of the two bunches are almost equal, which is the case at the beginning of the acceleration in the RCS. Therefore,
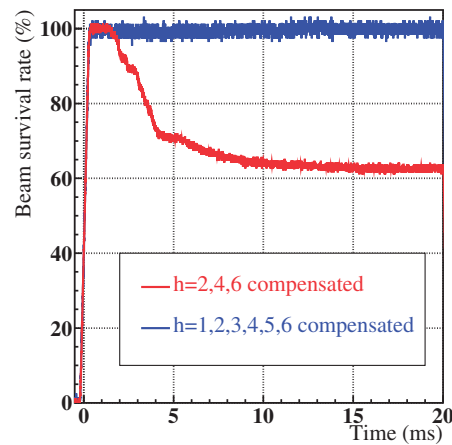
Fig. 1. Measured beam survival rate during acceleration of a 1 MW-eq. beam. The red line shows the case in which only the even harmonics of the beam loading are compensated. The blue line shows the case in which both odd and even harmonics are compensated.

it would appear reasonable to assume that applying beam loading compensation to the even harmonics only would be sufficient for high-intensity beam acceleration.

However, actual beam measurements contradict this assumption. Figure 1 shows the beam survival rate during acceleration for a 1 MW-eq. beam in the RCS. The red line represents the case in which only the $h = 2$, 4, and 6 harmonics are compensated, whereas the blue line represents the case in which all harmonics up to $h = 6$ are compensated. A large amount of beam loss occurs in the early acceleration phase when only the even harmonics are compensated. The fact that significant beam loss does not occur when the odd harmonics are also compensated suggests that the odd harmonics have a strong effect on the beam behavior.

From analyzing the beam measurements, it has been found that the odd harmonics are negligibly small at the beginning of the acceleration but they grow rapidly. If the total electric charges on the two bunches are almost the same, there are two conditions for the odd harmonics to appear: (1) the two bunches either approach or retreat from each other, and/or (2) each bunch has a different shape. The beam measurement suggests that both conditions appear simultaneously in the early acceleration phase.

One can see that when the width of the first bunch alternates between wide and narrow, the second bunch shows the opposite behavior. Furthermore, the bunches move apart and together synchronously. Consequently, once the odd harmonics appear, the odd harmonic wake voltages make the bunches more asymmetric, which increases the amplitude of the odd harmonics. We found that the potential well distortion caused by the odd harmonics can explain the alternating behavior of the bunch width and position.

We have also checked the bunch behavior by means of longitudinal particle tracking simulations, which reproduce the beam measurement results well. Phase space plots of the simulations show that the rf bucket alternately shrinks and expands. Such alternating behavior of the rf bucket induces an unwanted emittance growth that eventually leads to beam loss.

We describe the results of analyzing the beam measurements with and without the odd harmonic wake voltages. It is found that the simultaneous oscillations of the bunch positions and widths occur only with the odd harmonic wake voltages. Analysis of the rf potential well distortion shows good

Table 1. Parameters of the J-PARC RCS.

Injection energy	400 MeV
Extraction energy	3 GeV
Harmonic number	2
Number of bunches	2
Repetition rate	25 Hz
Acceleration period	20 ms
Number of protons	8.33×10^{13} ppp
Acceleration frequency	1.228–1.672 MHz
Momentum compaction factor	0.01198
Transition gamma	9.14 GeV

agreement with the bunch behavior. We also present the results of the particle tracking simulations in the form of the phase space information, which allows the beam loss mechanism to be understood.

The simultaneous oscillations caused by the odd harmonics are similar to a longitudinal bunched beam instability. We have also estimated the growth rate of the longitudinal instability caused by the cavity impedance, and the results suggest that the instability may not be the reason for the simultaneous oscillations observed in the RCS.

These results suggest that the minor Fourier components of the beam current should not be ignored in high-intensity proton synchrotrons.

2.   Beam measurements

The RCS accelerates protons from 400 MeV to 3 GeV in 20 ms. The parameters of the RCS are listed in Table 1. The 1 MW beam carries 8.33×10^{13} protons per pulse. The harmonic number is two, and two bunches are accelerated. The acceleration frequency varies widely from 1.228 to 1.672 MHz to follow the change of the velocity of the protons.

Figure 2 shows the typical rf voltage pattern and a synchronous phase. The red line in the upper graph is the fundamental acceleration voltage, and the blue line is the second harmonic voltage that flattens the bunch shape to alleviate the space charge effects [4,5]. The maximum fundamental acceleration voltage is 438 kV, which is generated by 12 rf cavities loaded with magnetic alloy (MA) cores [6–8]. Figure 3 shows the calculated synchrotron frequency, in which the acceleration voltage pattern in Fig. 2 is used. The horizontal axes represent the first 2 ms of the acceleration time.

2.1.   Bunch shape and position analysis

Wall current monitors (WCMs) are installed in the RCS to measure the longitudinal bunch shape. We investigate the bunch shape and position without the odd harmonic compensation in the following subsection, which corresponds to the red line in Fig. 1.

2.1.1.   Without odd harmonic compensation

Figures 4 and 5 show the beam harmonics during the 1 MW-eq. beam acceleration as determined by Fourier analysis of the WCM signals. The $h = 2$, 4, and 6 beam harmonics are shown in Fig. 4, and the $h = 1$, 3, and 5 harmonics are shown in Fig. 5. The horizontal axes represent the first 2 ms of the acceleration time. We define the time $t = 0$ as the minimum of the bending magnetic field, in which the bending magnet is driven by a sinusoidal wave form. The RCS uses a 0.5 ms duration multi-turn injection scheme that starts 0.25 ms before the minimum magnetic field.
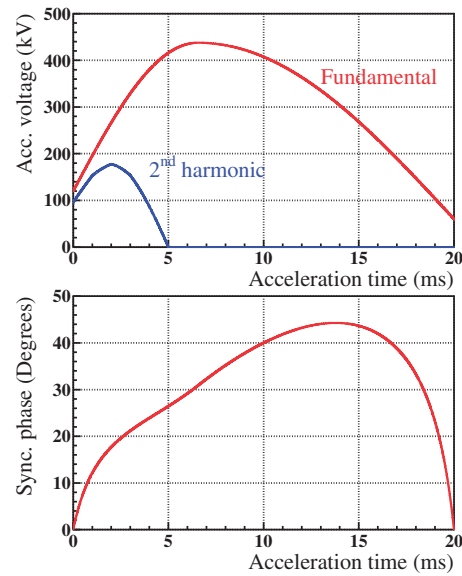
Fig. 2. Typical acceleration voltage pattern and synchronous phase of the RCS. In the upper graph, the red line indicates the fundamental acceleration voltage; the blue line indicates the second harmonic voltage.
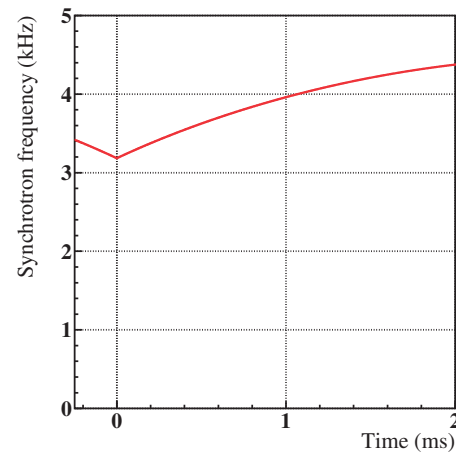
Fig. 3. Calculated synchrotron frequency using the acceleration voltage pattern in Fig. 2.

The two rf buckets at the RCS are filled with the injected beam during 307 turns, as indicated by the $h = 2$ harmonic in Fig. 4. The $h = 6$ harmonic is larger than the $h = 4$ one because the bunches are flattened by the second harmonic voltage ($h = 4$). Note that the beam loading compensation system cancels the wake voltages of the $h = 2$, 4, and 6 harmonics [2].

The odd harmonics are negligibly small during the multi-turn injection, after which they increase rapidly as shown in Fig. 5. The amplitudes of the odd harmonics peak at roughly 1.4 ms, corresponding to the start of the beam loss as shown in Fig. 1. This suggests that the odd harmonics play a key role in the beam loss.

Figure 6 shows a mountain plot of the bunches as measured by the WCM. The horizontal axis indicates the phase of the fundamental rf ($h = 2$), whereas the vertical axis indicates the acceleration time. This plot focuses on the time range of 0.5–1.5 ms, where the odd harmonics grow significantly. The first bunch is located around 0° phase, whereas the second one is located around 360° phase.
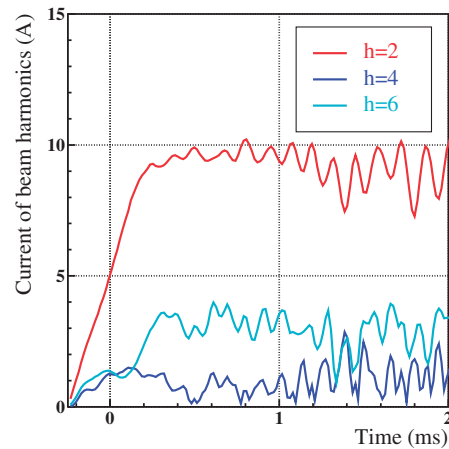
Fig. 4. Measured beam harmonics for $h = 2$, 4, and 6 during 1 MW-eq. beam acceleration without odd harmonic compensation. Red line: $h = 2$; blue line: $h = 4$; light-blue line: $h = 6$.
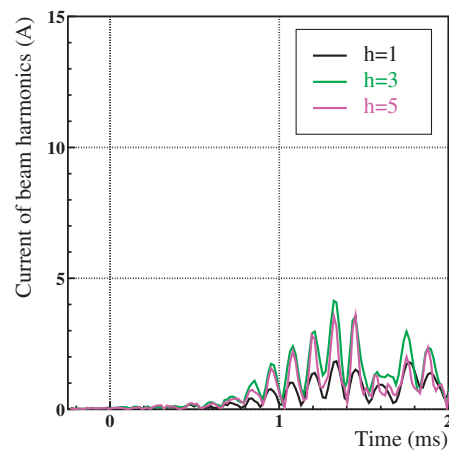
Fig. 5. Measured beam harmonics for $h = 1$, 3, and 5 during 1 MW-eq. beam acceleration without odd harmonic compensation. Black line: $h = 1$; green line: $h = 3$; pink line: $h = 5$.

The colors indicate the value of the WCM signal as shown at the right side in Fig. 6, with white indicating values over 20 A.

It is found from Fig. 6 that each bunch alternates between high and low bunch current. For example, the first bunch current is low and the second bunch current is high around 0.97, 1.21, and 1.45 ms, whereas the first bunch current is high and the second bunch current is low around 0.85, 1.1, and 1.34 ms. This alternating bunch peaking and flattening is associated with the growth of the odd harmonics.

Figure 7 shows the bunch shapes at 0.97, 1.1, 1.21, and 1.34 ms. The first bunch is wider than the second one at 0.97 and 1.21 ms, and vice versa at 1.1 and 1.34 ms. Figure 7 also gives information about the bunch center position. The bunches approach each other at 0.97 and 1.21 ms, when the first bunch is wider than the second one. In contrast, the bunches retreat from each other when the first bunch is narrower than the second one at 1.1 and 1.34 ms.

Figure 8 shows the variation in bunch width during acceleration. The horizontal axis represents the acceleration time, whereas the vertical axis represents the bunch width expressed as the phase of the fundamental rf ($h = 2$). The bunch width is evaluated from the root mean square of the WCM
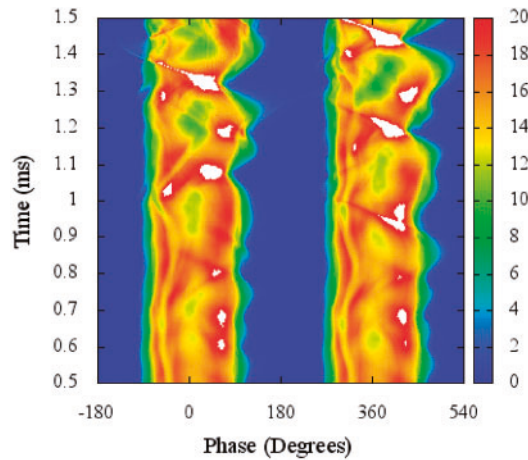
Fig. 6. Mountain plot of the first (left) and second (right) bunches measured by the WCM without the odd harmonic compensation.
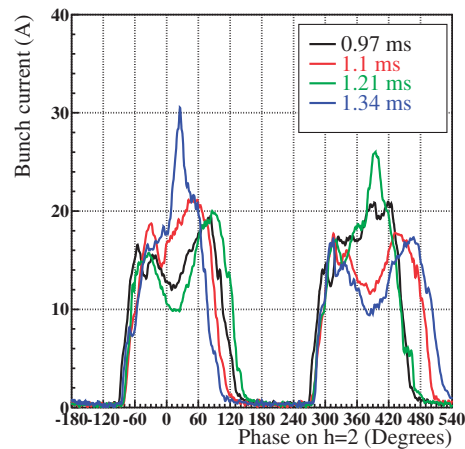
Fig. 7. Measured bunch shapes by the WCM at 0.97, 1.1, 1.21, and 1.34 ms without odd harmonic compensation. Black line: 0.97 ms; red line: 1.1 ms; green line: 1.21 ms; blue line: 1.34 ms.

signal. The red and blue lines indicate the first and second bunches, respectively. The alternating behavior starts around 0.5 ms and grows until 1.4 ms.

Figure 9 shows the variation of the center of the bunch electric charge during acceleration. On the vertical axis, $0°$ means that the bunch center is located at the zero-crossing phase of the fundamental rf ($h = 2$). The bunch centers drift from $0°$ with time because the bunch center nearly follows the synchronous phase. Furthermore, the large oscillations of both bunch centers in the early phase are because the RCS employs a momentum offset injection [5] that takes time to subside.

The bunches approach each other when the first bunch center is ahead of the center average, whereas they retreat from each other when the second bunch center is ahead. As can be seen clearly in Fig. 9, the bunches alternately approach and retreat; a so-called "π-mode" oscillation takes place.

Comparing Figs. 8 and 9, we see a correlation between the variations of the bunch width and center position. The bunches approach when the first bunch is wider than the second one, and vice versa. This correlation is considered to be due to the rf potential well distortion caused by the odd harmonic wake voltages. We discuss the potential well distortion in the following section.
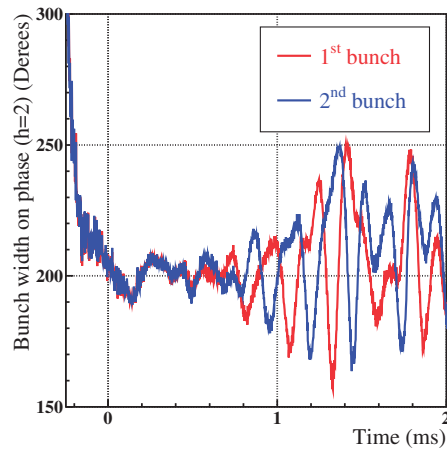
Fig. 8. Measured variation of bunch width during acceleration without odd harmonic compensation. The red and blue lines indicate the first and second bunches, respectively.
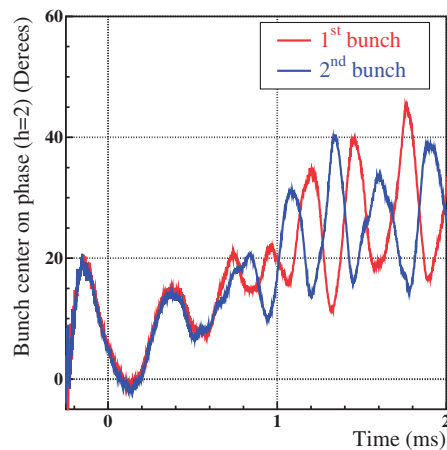
Fig. 9. Measured variation of bunch center position during acceleration without odd harmonic compensation. The red and blue lines indicate the first and second bunches, respectively.

2.1.2.   With odd harmonic compensation

For comparison, we investigate the WCM data in which the odd harmonics of $h = 1$, 3, and 5 are compensated, which corresponds to the blue line in Fig. 1. Unless stated otherwise, the colors and axis designations in the figures are the same as those for uncompensated odd harmonics.

Figures 10 and 11 show the beam harmonics during the 1 MW-eq. beam acceleration as obtained from analyzing the WCM signal. The beam harmonics for $h = 2$, 4, and 6 are shown in Fig. 10, and those for $h = 1$, 3, and 5 are shown in Fig. 11. Whereas a decrease in the $h = 2$ harmonic and a large oscillation after 1 ms were observed in Fig. 4, there are no such features in Fig. 10 for the even harmonics. Although the odd harmonics can be seen in Fig. 11, their amplitudes remain small because the beam loading compensation system suppresses the odd harmonic wake voltages.

Figure 12 shows a mountain plot of the bunches as measured by the WCM. Despite some small differences, the peaks and widths are fairly similar on both bunches. Figure 13 shows the bunch shape at the same time as Fig. 7; the widths and positions of the bunches are almost the same.

Figures 14 and 15 show the bunch width and center position, respectively, during acceleration; the data for the first bunch almost overlap those of the second one. In this case, the odd harmonics do not
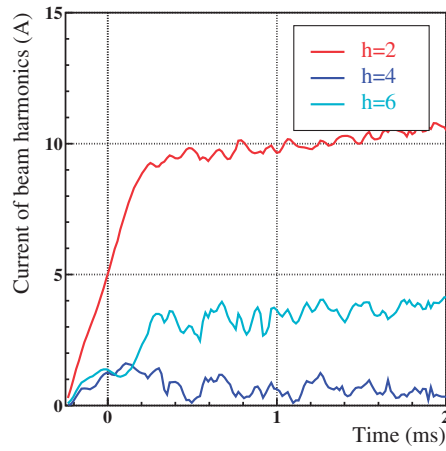
Fig. 10. Measured beam harmonics for $h = 2, 4$, and 6 during 1 MW-eq. beam acceleration with odd harmonic compensation. Red line: $h = 2$; blue line: $h = 4$; light-blue line: $h = 6$.
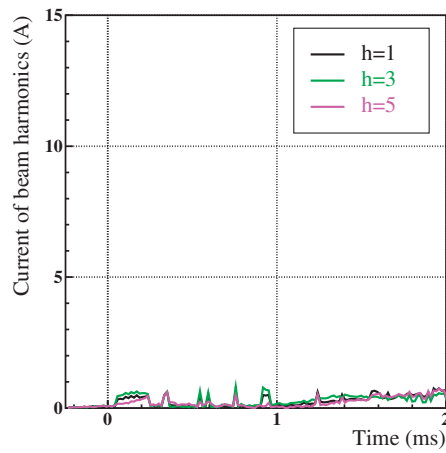
Fig. 11. Measured beam harmonics for $h = 1, 3$, and 5 during 1 MW-eq. beam acceleration with odd harmonic compensation. Black line: $h = 1$; green line: $h = 3$; pink line: $h = 5$.
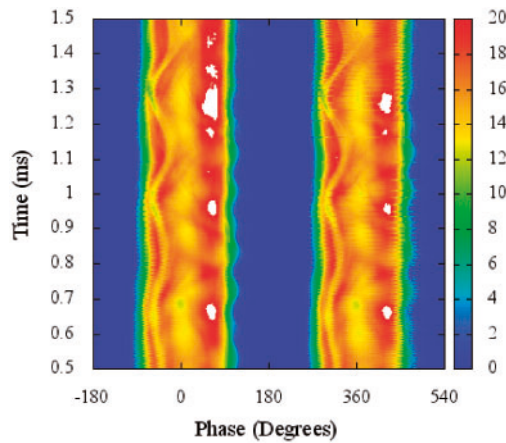
Fig. 12. Mountain plot of first (left) and second (right) bunches as measured by the WCM with odd harmonic compensation.
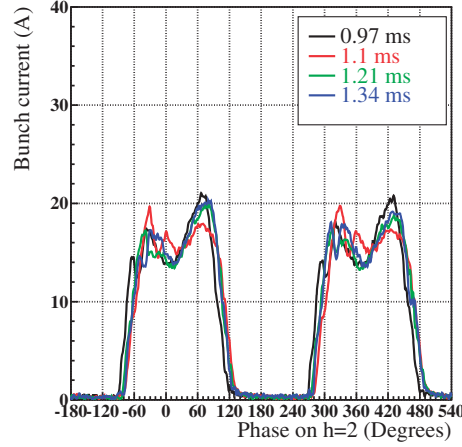
Fig. 13. Measured bunch shape obtained from WCM at 0.97, 1.1, 1.21, and 1.34 ms with odd harmonic compensation. Black line: 0.97 ms; red line: 1.1 ms; green line: 1.21 ms; blue line: 1.34 ms.
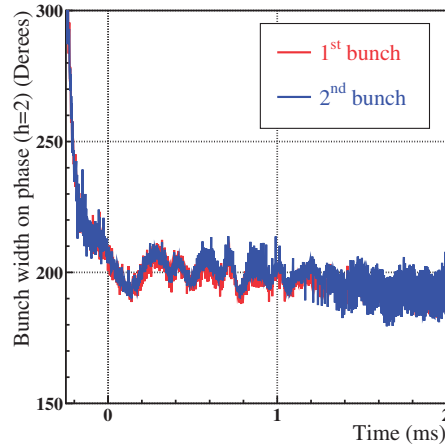
Fig. 14. Measured variation of the bunch width during acceleration with odd harmonic compensation. The red and blue lines indicate the first and second bunches, respectively.

tend to appear, which means that the beam loading compensation for the odd harmonics maintains the symmetry of the bunches.

2.2.   Analysis of potential well distortion

In order to investigate the oscillation of the bunch width and center position, we calculate the rf potential well including the wake voltages. We expect that the changes in bunch shape should follow the potential well variations closely [9]. We concentrate on the case without odd harmonic compensation because there are no special features with odd harmonic compensation.

The wake voltage V_b induced by the cavity impedance Z_{cav} is obtained by multiplying the beam current I_b by the cavity impedance,

$$V_{bh}(h\omega_{rev}) = Z_{cav}(h\omega_{rev}) \times I_b(h\omega_{rev}), \tag{1}$$

where ω_{rev} is the angular revolution frequency.

Figure 16 shows typical measurements of the rf cavity impedance. The RCS cavity has three acceleration gaps that are connected by busbars [10]; Fig. 16 shows the measurement for a single
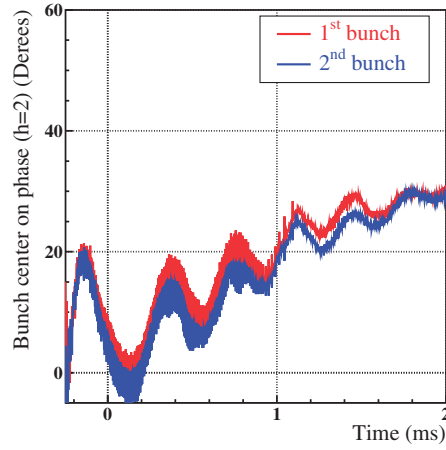
Fig. 15. Measured variation of the bunch center during acceleration with odd harmonic compensation. The red and blue lines indicate the first and second bunches, respectively.
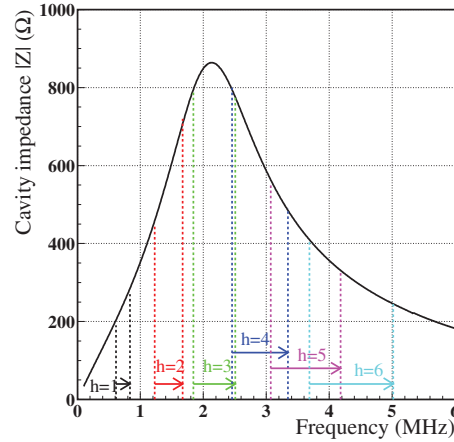
Fig. 16. Measured cavity impedance for a single gap. The frequency range of each harmonic from injection to extraction is also shown.

gap. The shut impedance is around $850\,\Omega$ per gap, the Q-value is around 1.5, and the resonance frequency is set to 2.1 MHz. In addition, the frequency range from injection to extraction is shown in Fig. 16 for each beam harmonic.

The condition under which the wake voltage is calculated is that the even harmonics of $h = 2, 4$, and 6 are canceled by the beam loading compensation system [2]. Hence, we consider only the odd harmonics in the range $h = 1$–7, after which all harmonics are included.

The amplitude of the wake voltage of each harmonic is calculated in the frequency domain using Eq. (1) and is then reproduced in the time domain by an inverse Fourier analysis as

$$V_{\mathrm{b}}(t) = \sum_{h=1}^{H_{\mathrm{b}}} V_{\mathrm{b}h} \sin(h\omega_{\mathrm{rev}}t + \phi_{\mathrm{b}h}), \tag{2}$$

where $\phi_{\mathrm{b}h}$ is the phase difference of the wake voltage for each harmonic and H_{b} is the upper limit of the harmonic to be calculated.

Figure 17 shows the results of calculating the wake voltages at 0.97, 1.1, 1.21, and 1.34 ms, which are the times used in Fig. 7. The wake voltages of $h = 2, 4$, and 6 are excluded, as mentioned
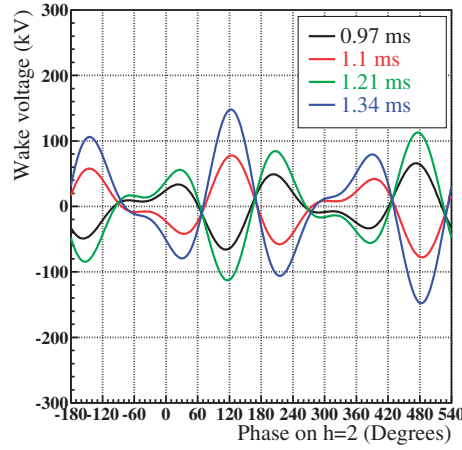
Fig. 17. Calculated wake voltages V_{b} at 0.97, 1.1, 1.21, and 1.34 ms without odd harmonic compensation. Black line: 0.97 ms; red line: 1.1 ms; green line: 1.21 ms; blue line: 1.34 ms.

above. It is found that the wake voltages at 0.97 and 1.21 ms have opposite phases to those at 1.1 and 1.34 ms. Furthermore, the wake voltage at each time has opposite phases on adjacent bunches. This is the most important characteristic of the odd harmonics, and is shown clearly by the potential well calculation described later.

The total voltage V_{t} that the bunch experiences is the sum of the fundamental acceleration voltage V_{h2}, the second harmonic voltage V_{h4} for bunch flattening, and the wake voltage V_{b}:

$$V_{\mathrm{t}}(\phi) = V_{\mathrm{h2}} \sin \phi + V_{\mathrm{h4}} \sin(2\phi + \phi_{\mathrm{h4}}) \tag{3}$$

$$- \sum_{h=1}^{H_{\mathrm{b}}} V_{\mathrm{b}h} \sin \left(\frac{h}{2}\phi + \phi_{\mathrm{b}h} \right),$$

where the phase ϕ is normalized on $h = 2$ and ϕ_{h4} is the phase difference from V_{h2}. The potential U_{t} of the total voltage is obtained as follows:

$$U_{\mathrm{t}}(\phi) = \frac{1}{V_{\mathrm{h2}}} \int_{\phi_{\mathrm{s}}}^{\phi} \left\{ V_{\mathrm{t}}(\phi') - V_{\mathrm{h2}} \sin \phi_{\mathrm{s}} \right\} d\phi', \tag{4}$$

where ϕ_{s} is the synchronous phase.

Figure 18 shows the result of calculating the potential well at 0.97, 1.1, 1.21, and 1.34 ms, which are the times in Fig. 7. As mentioned above, the wake voltages induced by $h = 2$, 4, and 6 harmonics are not considered. The results of calculating the potential suggest that the first bunch should be wide and the second one should be narrow at 0.97 and 1.21 ms, and vice versa at 1.1 and 1.34 ms. This is consistent with the changes in bunch width shown in Fig. 7.

Figure 18 also gives important information about the bunch center position. The potential wells of the first and second bunches are further apart at 1.1 and 1.34 ms than they are at 0.97 and 1.21 ms. This means that the bunches retreat from each other at 1.1 and 1.34 ms, whereas they approach each other at 0.97 and 1.21 ms. Again, this is also consistent with the variation in bunch center position shown in Fig. 7.

Figure 19 allows the potential well that arises from the wake voltages of $h = 1, 3, 5, 7$ and above to be compared with that from the wake voltages of $h = 1, 3$, and 5 only. The line in each graph indicates the calculated result for the wake voltages of $h = 1, 3, 5, 7$, and above, whereas the pink
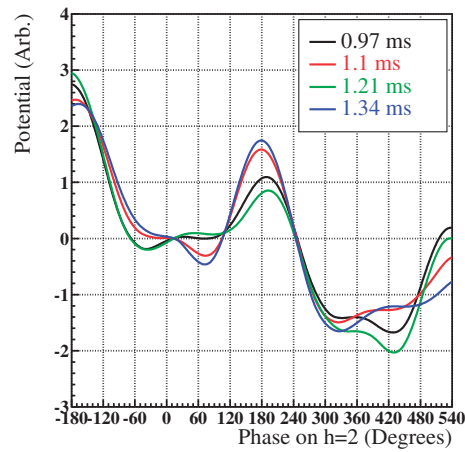
Fig. 18. Calculated results of potential formed by total voltage V_t at 0.97, 1.1, 1.21, and 1.34 ms without odd harmonic compensation. Black line: 0.97 ms; red line: 1.1 ms; green line: 1.21 ms; blue line: 1.34 ms.
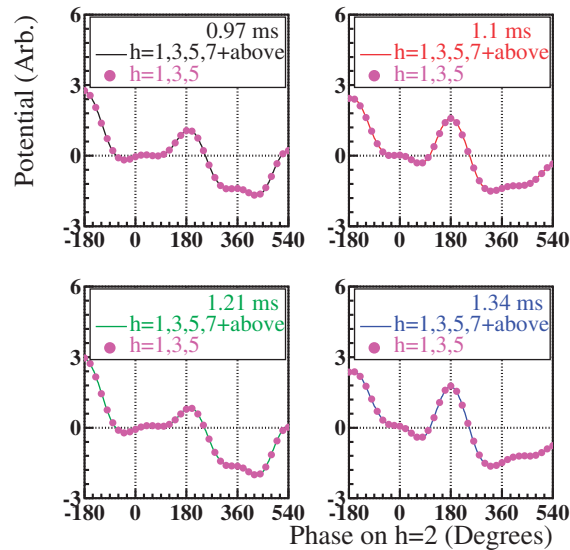
Fig. 19. Calculated results of the potential formed by the total voltage V_t at 0.97, 1.1, 1.21, and 1.34 ms. The solid line is the case in which the wake voltages of $h = 1, 3, 5, 7$, and above are included. The pink dots are the case in which the wake voltages of only $h = 1, 3$, and 5 are included.

dots indicate that with the wake voltages of $h = 1, 3$, and 5 only. Both sets of calculated results are almost the same, which means that the potential well distortion is caused mainly by the the odd harmonics up to $h = 5$ because the bandwidth of the cavity impedance covers those harmonics below $h = 6$.

Figure 20 shows the results of calculating the potential well width of each bunch during the acceleration. The calculation procedure is the same as that for the bunch width in Fig. 8, where the potential well shape is regarded as the bunch shape. The variation of the potential well width seen in Fig. 20 has the same tendency as that of the bunch width seen in Fig. 8. Although the amplitude is smaller than the case for bunch width, the same alternating behavior appears, and its timing is almost consistent with the bunch width case.

The same can be said for the variation of the center position. Figure 21 shows the results of calculating the potential well center of each bunch. Again, the calculation procedure is the same as
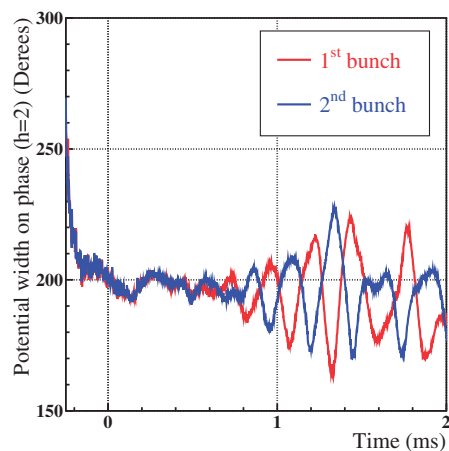
Fig. 20. Calculated results for the variation of the potential well width during acceleration without odd harmonic compensation. The red and blue lines indicate the potentials of the first and second bunches, respectively.
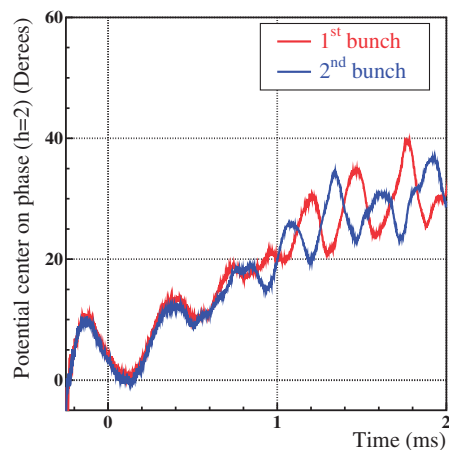
Fig. 21. Calculated results for the variation of the potential well center during acceleration without odd harmonic compensation. The red and blue lines indicate the potential of the first and second bunches, respectively.

that for the bunch center in Fig. 9. The variation of potential center seen in Fig. 21 has the same tendency as that of the bunch center in Fig. 9. We can see the "π-mode" oscillation, the timing of which is almost consistent with the bunch center case.

These calculated results suggest that the alternating potential well distortion is the origin of the variations in the bunch width and center position. The source of the simultaneous oscillations of the bunch width and center position is clearly the odd harmonics because the potential well distortion is caused by the odd harmonics up to $h = 5$, as shown in Fig. 19.

3. Particle tracking simulation

We check the beam behavior with the odd harmonic wake voltages by means of a longitudinal particle tracking simulation. The simulation code was originally developed for the J-PARC synchrotrons [5], and it simulates not only basic longitudinal particle motion but also the multi-turn injection, the wake voltages, and a space charge effect.
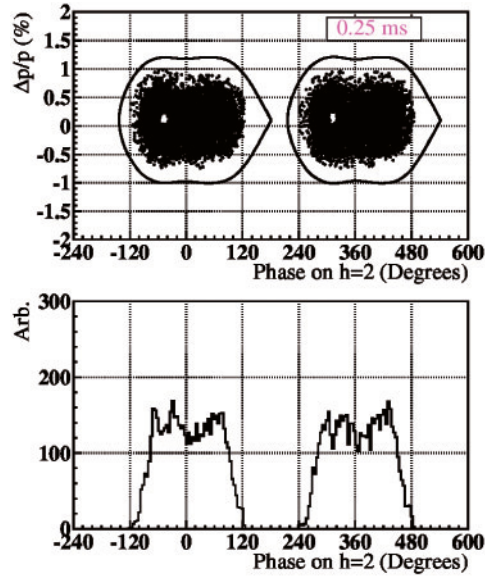
Fig. 22. Particle distribution in the phase space (upper graph) and bunch shape (lower graph) at the end of the multi-turn injection.

The simulation is performed under the same conditions as those of the beam measurements. The code uses the acceleration voltage pattern as shown in Fig. 2 and the bunch electric charge for the 1 MW-eq. beam. The other parameters are also the same as listed in Table 1. The injected beam has a rectangular shape for the longitudinal direction with 489 ns width, and the momentum spread is 0.14%. This chopped beam is injected 306 times during 500 μs multi-turn injection.

The cavity impedance is assumed to be an *LCR* parallel resonant circuit. This is expressed with a shunt impedance R_{sh}, a Q-value, and an angular resonant frequency ω_r as follows:

$$Z_{cav} = \frac{R_{sh}}{1 + iQ\left(\dfrac{\omega_r}{\omega} - \dfrac{\omega}{\omega_r}\right)}, \tag{5}$$

where ω is an angular frequency. The cavity resonance frequency of 2.1 MHz and $Q = 1.5$ are used for the simulation. The impedance shown in Fig. 16 corresponds to one acceleration gap. The beam sees a 36 times larger impedance because each cavity has 3 acceleration gaps, and 12 cavities are installed in the RCS. Consequently, R_{sh} becomes 30.6 kΩ.

An initial particle distribution of the injected beam is generated randomly, and the bunches are formed through the multi-turn injection. Figure 22 shows the particle distribution and the bunch shape at the end of the multi-turn injection. The differences between the bunches are small, and thus the odd harmonics are small until this time.

Unless stated otherwise, the colors and axis designations in the figures are the same as those in the beam measurement case.

3.1. Bunch shape and position analysis

Figure 23 shows the results of simulating the beam survival rate. A large amount of beam loss is observed in the case that the odd harmonics of $h = 1, 3$, and 5 are not compensated. This is quite similar to the beam measurements as shown in Fig. 1. We concentrate on the case without odd harmonic compensation because there are no special features with odd harmonic compensation.
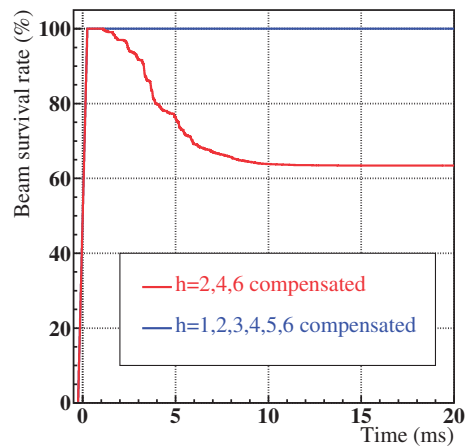
Fig. 23. Simulation results of beam survival rate during acceleration of 1 MW-eq. beam. The red line indicates the case in which only the even harmonics of the beam loading are compensated. The blue one indicates the case in which compensation is applied for both even and odd harmonics.
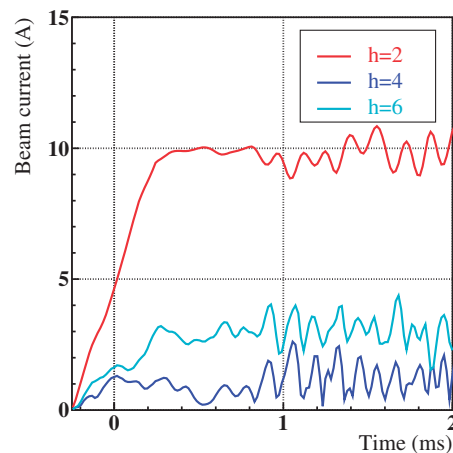
Fig. 24. Simulation results of beam harmonics for $h = 2, 4$, and 6 during 1 MW-eq. beam acceleration without odd harmonic compensation. Red line: $h = 2$; blue line: $h = 4$; light-blue line: $h = 6$.

Figures 24 and 25 show the beam harmonics for $h = 2, 4$, and 6 and $h = 1, 3$, and 5, respectively, during acceleration. Comparing Figs. 25 and 5, the appearance of the odd harmonics in the simulation is almost the same as that in the beam measurements, although the odd harmonics appear slightly earlier in the simulation than they do in the measurements. This is also observed in the beam survival rate in Fig. 23; the beam loss starts slightly earlier in the simulation.

Figure 26 shows the bunch shape at 0.84, 0.99, 1.13, and 1.24 ms. Again, the alternating behavior of the bunch width can be seen, as in Fig. 7. The first bunch becomes wider than the second one at 0.84 and 1.13 ms, and vice versa at 0.99 and 1.24 ms. Figure 26 also gives information about the bunch center position. The bunches approach each other at 0.84 and 1.13 ms when the first bunch is wider than the second one. In contrast, the bunches retreat from each other when the first bunch is narrower than the second one at 0.99 and 1.24 ms.

Figures 27 and 28 show the bunch width and the center position, respectively, during acceleration. The alternating behavior of bunch width and center position is again observed, as in Figs. 8 and 9.
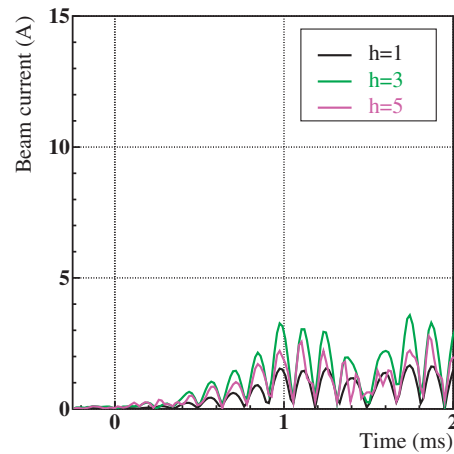
Fig. 25. Simulation results of beam harmonics for $h = 1, 3$, and 5 during 1 MW-eq. beam acceleration without odd harmonic compensation. Black line: $h = 1$; green line: $h = 3$; pink line: $h = 5$.
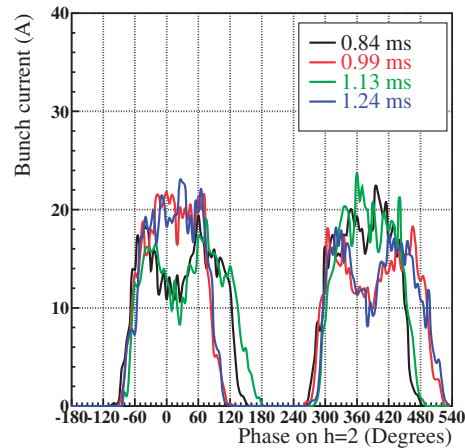
Fig. 26. Simulation results of bunch shape at 0.84, 0.99, 1.13, and 1.24 ms. Black line: 0.84 ms; red line: 0.99 ms; green line: 1.13 ms; blue line: 1.24 ms.

Furthermore, there is correlation between the variation of the bunch width and the bunch center position in the simulation. This is also similar to the beam measurements.

3.2. Analysis of potential well distortion

The potential well distortion is also calculated to verify the simulation. The calculation procedure is the same as in the beam measurement case. Unless stated otherwise, the colors and axis designations in the figures are the same as those in the beam measurement case.

Figure 29 shows the results of simulating the potential well at 0.84, 0.99, 1.13, and 1.24 ms, which are the times in Fig. 26. The results indicate that the first bunch should be wide and the second one should be narrow at 0.84 and 1.13 ms, and vice versa at 0.99 and 1.24 ms. This is consistent with the variation in bunch width shown in Fig. 26.

Furthermore, the potential wells of the first and second bunches are further apart at 0.99 and 1.24 ms than they are at 0.84 and 1.13 ms. This means that the bunches retreat from each other at 0.99 and 1.24 ms, whereas they approach each other at 0.84 and 1.13 ms. Again, this is consistent with the
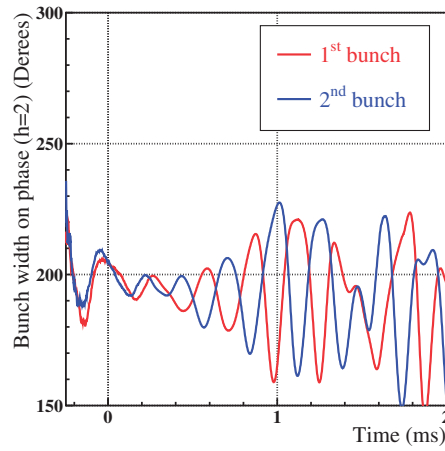
Fig. 27. Simulation results of the bunch width during acceleration without odd harmonic compensation. The red and blue lines indicate the first and second bunches, respectively.
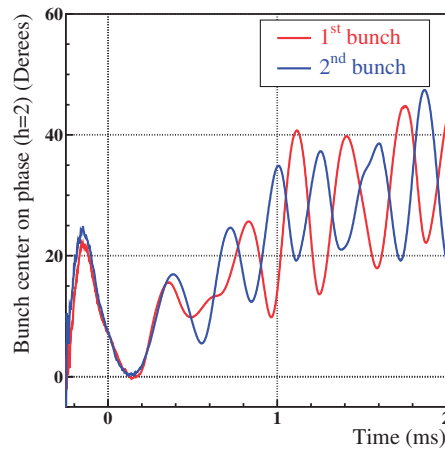
Fig. 28. Simulation results of bunch center during acceleration without odd harmonic compensation. The red and blue lines indicate the first and second bunches, respectively.
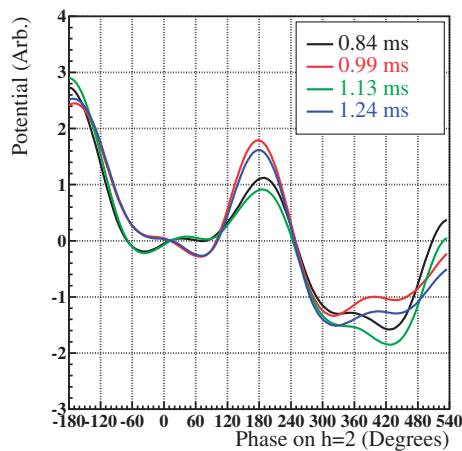
Fig. 29. Simulation results of potential well formed by total voltage V_{t} at 0.84, 0.99, 1.13, and 1.24 ms without odd harmonic compensation. Black line: 0.84 ms; red line: 0.99 ms; green line: 1.13 ms; blue line: 1.24 ms.
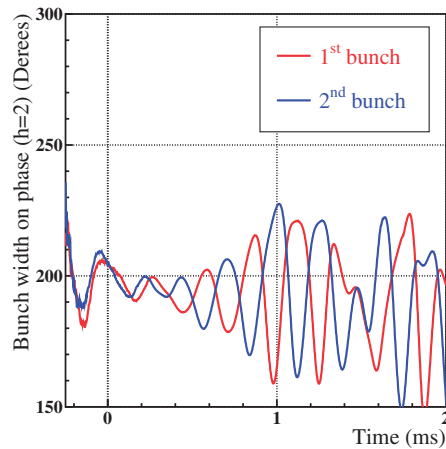
Fig. 30. Simulation results of the potential width during acceleration without odd harmonic compensation. The red and blue lines indicate the potentials of the first and second bunches, respectively.
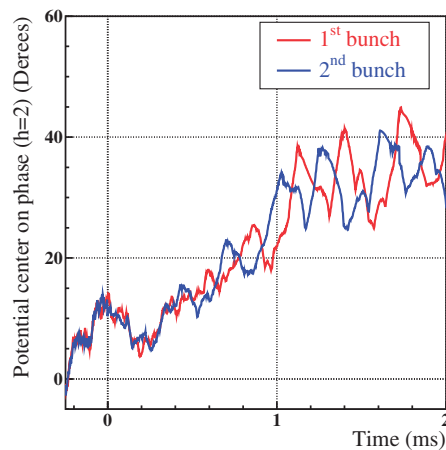
Fig. 31. Simulation results of the potential center position during acceleration without odd harmonic compensation. The red and blue lines indicate the potential of the first and second bunches, respectively.

variation in bunch center position shown in Fig. 26. The alternating behavior of the potential well width and center position is also seen in the simulation, as in the measurement case in Fig. 18.

Figures 30 and 31 show the potential well width and center position during the acceleration. The alternating behavior is again observed in the potential as in Figs. 27 and 28; the timings of the oscillations of the potential width and center position are also consistent with those of the bunch case.

The above results support agreement between the particle tracking simulation and the beam measurement. In the following subsection, we see phase space plots with the odd harmonic wake voltages to understand the particle motion under the rf bucket distortion.

3.3. Particle motion in phase space

Figure 32 shows the particle distribution and the rf bucket in the phase space at 0.84 ms, which corresponds to the black lines in Figs. 26 and 29. One can see that the odd harmonic wake voltages cause the first bucket to shrink and the second one to expand. All the particles remain in the rf buckets. Figure 33 shows the particle distribution and the rf bucket in the phase space at 0.99 ms,
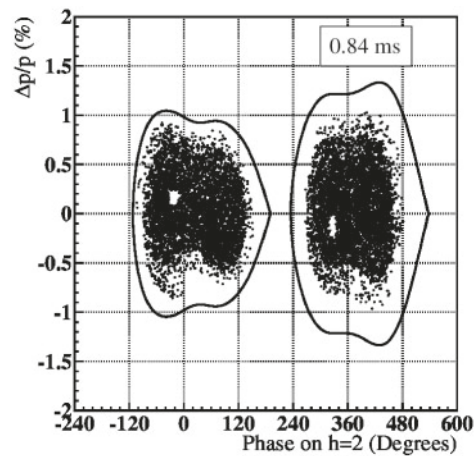
Fig. 32. Simulated particle distribution and the rf bucket in the phase space at 0.84 ms. The odd harmonics cause the first bucket to shrink and the second one to expand.

which corresponds to the red lines in Figs. 26 and 29. In this case, the first bucket expands and the second one shrinks, and some particles in the second bucket reach close to the edge of the rf bucket.

Figure 34 shows the case at 1.13 ms, which corresponds to the green lines in Figs. 26 and 29. One can see that the first bucket shrinks again, and now some particles escape. Furthermore, the second bucket expands, and some particles make a tail that would have settled near the edge of the second bucket in Fig. 33.

Figure 35 shows the case at 1.24 ms, which corresponds to the blue lines in Figs. 26 and 29. In this case, the first bucket expands again, and some particles make a tail that would have settled near the edge of the first bucket in Fig. 34. The second bucket shrinks again, and the tail part in Fig. 34 is already outside the bucket.

This repetitive shrinking and expanding distorts the particle distribution and brings some particles to the outside of the buckets. The particle tracking simulation reveals the mechanism whereby the odd harmonics cause beam loss.

For comparison, the simulation is also performed for the case in which the odd harmonics of $h = 1$, 3, and 5 are compensated, which corresponds to the blue line in Fig. 23. The particle distribution and the rf bucket are shown in Fig. 36. This is the representative result at 1.24 ms, and we confirm that the particle distribution is always stable.

4.   Discussion

The simultaneous oscillations caused by the odd harmonic beam loading are similar to the beam instability. For comparison, we discuss well-known longitudinal bunched beam instabilities.

4.1.   Stability criteria using phasor diagram

Stability analysis using phasor diagrams [11–13] can be applied to high-intensity beam acceleration in the RCS. Without rf-feedforward compensation, the relative loading factor is considerably higher than 2 at the beginning of acceleration. However, thanks to the rf-feedforward compensation [2,3], the beam loading is well compensated and the relative loading factor is kept close to zero. Therefore, the condition is within the stable region.
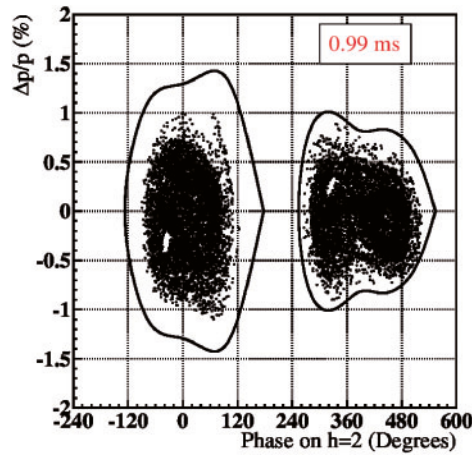
Fig. 33. Simulated particle distribution and the rf bucket in the phase space at 0.99 ms. The odd harmonics cause the first bucket to expand and the second one to shrink.
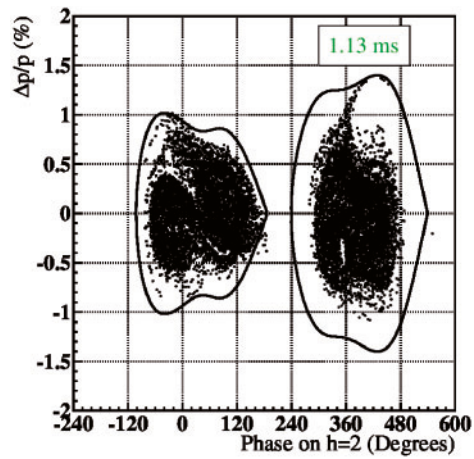
Fig. 34. Simulated particle distribution and the rf bucket in the phase space plot at 1.13 ms. The odd harmonics cause the first bucket to shrink and the second one to expand.
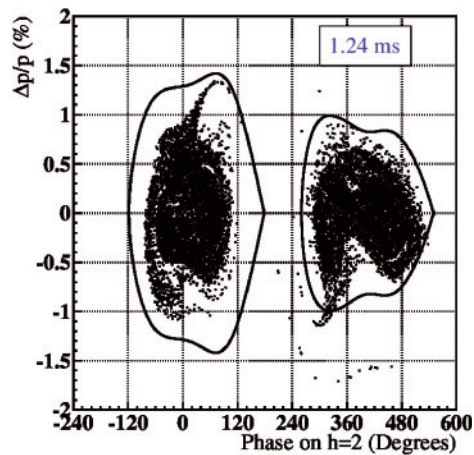
Fig. 35. Simulated particle distribution and the rf bucket in the phase space plot at 1.24 ms. The odd harmonics cause the first bucket to expand and the second one to shrink.
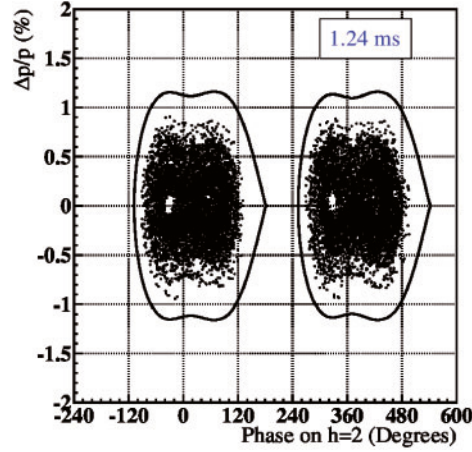
Fig. 36. Simulated particle distribution and the rf bucket in the phase space at 1.24 ms. The odd harmonics wake voltage are canceled in this case.

Table 2. Parameters for the instability calculation.

e	Elementary electric charge	
I_a	Average circulating bunch current	4.1 A
η	Slippage factor	-0.48
β	Relativistic factor	0.71
E_0	Total energy of proton	1.338 GeV
ν_{s0}	Synchrotron tune	0.0052
$\hat{\tau}$	Bunch half-width	280 ns
ω_{rev}	Angular revolution frequency	$2\pi \times 0.614$ MHz

4.2. Robinson instability

We can estimate the effect from the higher harmonics by the instability theory using a coupling impedance [14–17]. The growth rate τ_m^{-1} of the longitudinal Robinson instability based on the linearized Vlasov equation using a water bag model is expressed as

$$\tau_m^{-1} \simeq \frac{meI_a\eta}{4\pi\beta^2 E_0\nu_{s0}} \sum_{p=-\infty}^{\infty} \omega' \cdot \Re\left[Z_L(\omega')\right] \cdot \left[\frac{J_m(\omega'\hat{\tau})}{\omega'\frac{\hat{\tau}}{2}}\right]^2, \tag{6}$$

where m is the mode number of the bunch motion: $m = 1$ is dipole mode, $m = 2$ is quadrupole mode, and so on. J_m is the Bessel function of the first kind, and

$$\omega' = (p + m\nu_{s0})\omega_{rev}, \tag{7}$$

where p is an integer number. The other parameters in Eqs. (6) and (7) are listed in Table 2, in which the calculated values at the injection are also shown. $\Re[Z_L]$ is the real part of the longitudinal impedance Z_L, and the cavity impedance Z_{cav} in Eq. (5) for the resonance frequency of 2.1 MHz is substituted into Z_L.

The calculated growth rate is shown in Fig. 37. The horizontal axis indicates the mode number and the vertical axis indicates the growth rate. A positive sign means the instability grows, and a negative one means it should be damped. The growth rate above 500 Hz is expected from the beam
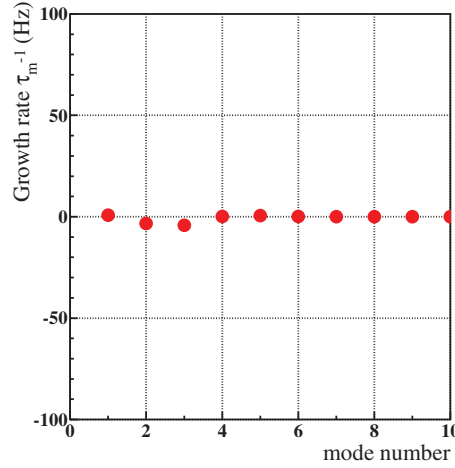
Fig. 37. Calculated growth rate for the Robinson instability of *m*-mode.

measurement, because the beam loss occurs at less than 2 ms. However, the growth rate is smaller than the expected value, and the Robinson instability does not seems to occur in the RCS.

4.3. Coupled bunch instability

Next, we check the growth rate of the coupled bunch instability. The growth rate τ_{m}^{-1} caused by M bunches based on the linearized Vlasov equation using the water bag model is expressed as

$$\tau_{\mathrm{m}}^{-1} \simeq \frac{m M e I_{\mathrm{a}} \eta}{4 \pi \beta^2 E_0 \nu_{\mathrm{s}0}} \sum_{p=-\infty}^{\infty} \omega' \cdot \Re \left[Z_{\mathrm{L}}(\omega') \right] \cdot \left[\frac{J_{\mathrm{m}}(\omega' \hat{\tau})}{\omega' \frac{\hat{\tau}}{2}} \right]^2 . \tag{8}$$

The picking up frequencies are different from the Robinson instability,

$$\omega' = (Mp + \mu + m\nu_{\mathrm{s}0})\omega_{\mathrm{rev}}. \tag{9}$$

μ is the coupled bunch mode number, and the RCS has only two modes: $\mu = 0$ is "in-phase" and $\mu = 1$ is "opposite-phase." The parameters in Table 2 are also used for the growth rate calculation.

The calculated growth rate is shown in Figs. 38 and 39. Figure 38 is the case of the $\mu = 0$ mode, and Figure 39 is the case of the $\mu = 1$ mode. Although the growth rate of the $\mu = 0$ mode is slightly larger than the case of the Robinson instability, it is still smaller than the expected value. The beam measurement with the odd harmonic beam loading indicates that the bunch position motion corresponds to $\mu = 1$ mode as shown in Fig. 9. However, the growth rate of the $\mu = 1$ mode is very small. These results suggest that the coupled bunch instability cannot explain the bunch behavior caused by the odd harmonics in the RCS.

4.4. Bucket distortion

The beam measurement and the simulation suggest that the odd harmonics grow rapidly and cause beam loss. The most distinctive feature is that the alternating behavior of the bunch width is observed. This is different from a quadrupole oscillation in the longitudinal motion, and the odd harmonics directly change the rf bucket shape as shown in Figs. 32–35. The oscillation of the bunch center position is promoted by the alternating change of the bunch width, and the change of the bunch width also promotes the change of the bunch position.
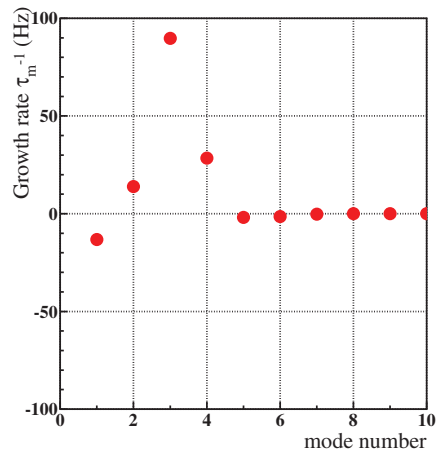
Fig. 38. Calculated growth rate for the coupled bunch instability of the $\mu = 0$ mode.
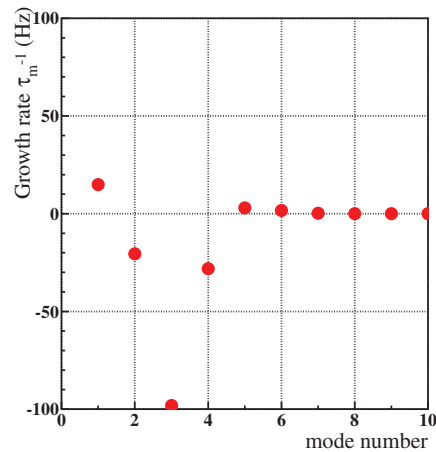
Fig. 39. Calculated growth rate for the coupled bunch instability of the $\mu = 1$ mode.

There seem to be some conditions where the alternating behavior continues. The phase of the odd harmonic wake voltages is considered as a key issue because the odd harmonics do not tend to increase when the resonance frequency of the rf cavity is set to 1.7 MHz [1], whereas we mainly describe the case of 2.1 MHz in this article. Further investigations are needed to determine the conditions for which this kind of the behavior occurs.

The present investigation has demonstrated that the minor beam harmonics sometimes grow and cause significant beam loss in the high-intensity beam operation. A straightforward solution to avoid this behavior is compensating the beam loading not only for the even harmonics but also for the odd harmonics, as shown in Sect. 2.1.2. Although we described the simplest case in the RCS, that is, two rf buckets are filled with the two bunches, this kind of behavior may be observed for the case of more bunches. The beam loading compensation system should be concerned with the minor harmonics in high-intensity beam operation.

5.   Conclusion

We have investigated the effect of odd harmonics on the beam loading at the J-PARC RCS. Although the odd harmonics are very small at the beginning, they increase rapidly and then cause beam

loss. There is good agreement between beam measurements and the particle tracking simulations, both of which suggest that the potential well distortion caused by the odd harmonics promotes the simultaneous oscillations of bunch shape and position. The phase space plots in the simulation suggest that the rf bucket shrinking and expanding disturb the particle distribution and finally cause the beam loss. This phenomenon cannot be explained by the ordinary longitudinal bunched beam instability mechanism because the estimated growth rates are much smaller than the expected value from the beam measurement.

Since this behavior can be suppressed in principle by compensating the odd harmonics of the beam loading, the beam loading compensation system should manage such minor harmonics.

References

[1] H. Hotchi et al., Proc. Int. Particle Accelerator Conf., p. 592 (2016).
[2] F. Tamura, M. Yamamoto, C. Ohmori, A. Schnase, M. Yoshii, M. Nomura, M. Toda, T. Shimada, K. Hara, and K. Hasegawa, Phys. Rev. ST Accel. Beams **14**, 051004 (2011).
[3] F. Tamura, C. Ohmori, M. Yamamoto, M. Yoshii, A. Schnase, M. Nomura, M. Toda, T. Shimada, K. Hasegawa, and K. Hara, Phys. Rev. ST Accel. Beams **16**, 051002 (2013).
[4] F. Tamura et al., Phys. Rev. ST Accel. Beams **12**, 041001 (2009).
[5] M. Yamamoto et al., Nucl. Instr. and Meth. A **621**, 15 (2010).
[6] M. Yamamoto et al., Proc. European Particle Accelerator Conf., p. 1322 (2006).
[7] M. Yamamoto et al., Proc. Particle Accelerator Conf., p. 1532 (2007).
[8] M. Nomura, A. Schnase, T. Shimada, F. Tamura, M. Yamamoto, K. Hara, K. Hasegawa, C. Ohmori, M. Toda, and M. Yoshii, Nucl. Instr. and Meth. A **668**, 83 (2012).
[9] A. Hofmann and F. Pedersen, Proc. 8th Particle Accelerator Conf., p. 592 (1979).
[10] M. Yamamoto, M. Nomura, T. Shimada, F. Tamura, K. Hara, K. Hasegawa, C. Ohmori, M. Toda, M. Yoshii, and A. Schnase, Nucl. Instr. and Meth. A **835**, 119 (2016).
[11] K. W. Robinson, SLAC-49 (1965). doi: 10.2307/321960
[12] P. B. Wilson, Proc. 9th Int. Conf. on High Energy Accelerators, p. 57 (1974).
[13] F. Pedersen, Proc. 6th Particle Accelerator Conf., p. 1906 (1975).
[14] F. Sacherer, CERN/SI-BR/72-5 (1972).
[15] F. Sacherer, Proc. 7th Particle Accelerator Conf., p. 1393 (1977).
[16] A. W. Chao, SLAC-PUB-2946 (1982).
[17] T. Suzuki, Y. H. Chin, K. Satoh, Part. Accel. **13**, 179 (1983).